CrystEngComm

Accepted Manuscript

ROYAL SOCIETY OF CHEMISTRY

www.rsc.org/crystengcomm

Cite this: DOI: 10.1039/c0xx00000x

www.rsc.org/xxxxxx

ARTICLE TYPE

Hydrothermal synthesis of single-crystalline tetragonal perovskite $PbTiO_3$ nanosheets with dominant (001) or (111) facets

Gang Xu,*[a,b] Xiaoqiang Huang,[a] Vladimir Krstic,[b] Shuquan Chen,[b] Xin Yang,[a] Chunying Chao,[a] Ge Shen,[a] Gaorong Han,[a]

Received (in XXX, XXX) Xth XXXXXXXXX 20XX, Accepted Xth XXXXXXXXX 20XX

DOI: 10.1039/b000000x

Single-crystalline tetragonal peroskite $PbTiO_3$ nanosheets are synthesized via hydrothermal route assisted with $NaNO_3$ and KNO_3, respectively. Due to the difference in electronegativity, Na+ ions are fastened on (001) planes, whereas K+ ions on (111) planes, resulting in the PbTiO3 nanosheets dominant with (001) or (111) facets, respectively.

Lead titanate perovskite, $PbTiO_3$, has a distorted perovskite structure below about 490 °C and consequently displays a spontaneous polarization. The polarization direction of the $PbTiO_3$ crystal switches between two stable polarization states corresponding to the positive and negative electric bias. This particular feature makes $PbTiO_3$ a candidate for nonvolatile ferroelectric random-access memories (NVFRAMs). [1] Previous researches have demonstrated that perovskite $BaTiO_3$ nanowires as small as 10 nm in diameter retain ferroelectricity. [2,3] Despite the storage density achieved 10^9 bit/cm^2 in virtue of the bistable polarization states of the ferroelectric $BaTiO_3$ nanowires, [2] it is necessary to look for nonvolatile memory devices with higher storage density to meet the requirement of the practice and the miniaturization. Whereas two-dimensional (2D) nanostructures can have high tap density by overlapping assembly compared to one-dimensional nanostructures, even higher storage density may be possible to realize by ferroelectric nanosheets.

Since the discovery of graphene, [9, 10] 2D nanosturctures have attracted considerable attentions from the scientific community because of their potential application. Up to now, a variety of layered metal oxides, chalcogenides, and hydroxides have been exfoliated into inorganic nanosheets or a unique class of molecularly thin 2D crystallites. [4-8] However, the preparation of the 2D nanostructures with 3D rigid crystal framework, such as perovskite oxide 2D nanostructures, is still a challenge.

Hydrothermal technique is an aqueous-based precipitation route. The crystal nucleation and growth can be easily controlled over by tuning the hydrothermal conditions. [11-13] In our previous researching work, single-crystalline tetragonal perovskite lead zirconate tianate (PZT) nanorods and nanowires have been synthesized via a simple conventional hydrothermal route assisted with polymer. [11] The preferential adsorption of PVA and PAA molecules on (100) and (010) planes results in the single-crystalline tetragonal perovskite lead zirconate tianate (PZT) nanorods and nanowires along with the direction of [001]. Herein, the synthesis of $PbTiO_3$ nanosheets with a thickness of about 10 nm and a lateral size of about 400 nm was successfully realized via a conventional hydrothermal method assisted with $NaNO_3$ or KNO_3 as additives. Due to the difference in electronegativity between element Na and K, the preferentially faster combination of Na^+ ions with the O^{2-} ions situated at (001) leads to the $PbTiO_3$ nanosheets with dominant (001) facets, while that of K^+ ions with the O^{2-} ions situated at (111) results in the $PbTiO_3$ nanosheets with dominant (111) facets. The corresponding EDS spectrums (Fig. S1) indicate that the $PbTiO_3$ nanosheets consist of Pb Ti, and O, furthermore, the Pb/Ti ratio is about 1:1, agreeing well with the nominal composition of $PbTiO_3$.

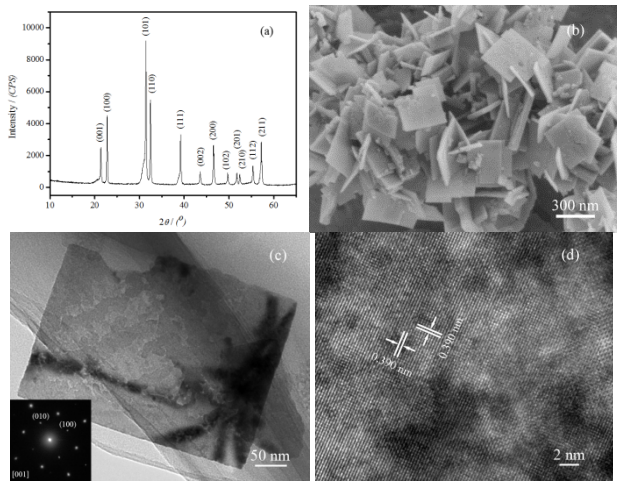

Fig. 1 XRD pattern and (b) SEM image of the hydrothermally synthesized perovskite lead titanate nanosheets assisted with $NaNO_3$ as additives, (c) TEM image of one single $PbTiO_3$ nanosheet, (d) HRTEM image of the as-prepared $PbTiO_3$ nanosheets. Inset in (c) shows the SAED pattern caught from the whole single $PbTiO_3$ nanosheet

Fig. 1a shows the XRD pattern of the synthesized $PbTiO_3$ samples assisted with $NaNO_3$. All diffraction peaks can be assigned to tetragonal perovskite $PbTiO_3$ phase with the lattice parameter a=b=0.390 nm and c=0.415 nm, in agreement with the reported data of JCPDS No. 06-0452, confirming that the obtained samples are of tetragonal perovskite $PbTiO_3$ phase without any impurities. The strong and sharp diffraction peaks suggest that the as-prepared products are well crystallized. However, a detailed examination reveals that there is a broadened shoulder accompanying each diffraction peak. An overview SEM image (Fig. S2) illustrates that the as-prepared perovskite $PbTiO_3$

samples consist of nanosheets and cubic crystals with faint edges. The magnified SEM image shown in Fig. 1b reveals that the thickness of the $PbTiO_3$ nanosheets is about 10 nm and the lateral size is about 400 nm. Moreover, a few $PbTiO_3$ nanoparticles are observed. Representative TEM and HRTEM images of a single $PbTiO_3$ nanosheet are shown in Fig. 1c and d, respectively. From the TEM image, some dark muscles are observed, implying inherent lattice strain occurrence in the formed single-crystal $PbTiO_3$ nanosheets. The broadened shoulder observed in the XRD pattern can be ascribed to the cooperation of the strain involved in the single-crystal $PbTiO_3$ nanosheets and the $PbTiO_3$ nanoparticles. Two sets of lattice fringes with 0.390 intervals, which agree well with the spacing of (100) and (010) planes, are identified from the HRTEM image shown in Fig. 1d. Whereas the two sets of lattice fringes are perpendicular to each other and a regular SAED pattern (inset in Fig. 1c) along [001] direction is taken from the corresponding whole single nanosheet, it can be concluded that the obtained $PbTiO_3$ nanosheets are single-crystalline and dominant with (001) facets.

However, as the hydrothermal synthesis is carried out without any $NaNO_3$ additive the synthesized $PbTiO_3$ samples are of cubic particles with faint facets (Fig. S3). It is evident that the addition of $NaNO_3$ induces the single-crystalline tetragonal perovskite $PbTiO_3$ nanosheets with dominant (001) facets.

According to the formation mechanism of oxides from hydroxides under the hydrothermal conditions, [14] the tetragonal perovskite $PbTiO_3$ is formed by dehydrating condensation of the lead and titanium hydroxides. In view of the reversibility of the dehydration of the hydroxides, it is reasonable to propose that the P25-TiO_2 used as raw material firstly converts to titanium hydroxides, and then, combines with lead hydroxides to form lead titanate species by undergoing a dehydrating condensation process under the hydrothermal conditions. As the formed lead titanate species accumulate to a moderate concentration, a number of tetragonal perovskite $PbTiO_3$ crystal nuclei larger than the critical size appear. These nuclei then grow by incorporating with the additional lead titanate species to form tetragonal perovskite $PbTiO_3$ crystals. Because the hydrothermally synthesized $PbTiO_3$ cubic particles reflect the intrinsic symmetry of the lattice, it is argued that the hydrothermal reaction without the presence of $NaNO_3$ occurs at equilibrium. [15] When $NaNO_3$ is introduced into the hydrothermal system, the equilibrium is disturbed. In aqueous solution $NaNO_3$ ionizes and releases Na^+ and NO_3^- ions. Due to the reversibility of the ionization, the released Na^+ ions trend to combine with the O^{2-} ions situated at the surfaces of the formed $PbTiO_3$ crystals not only the O^{2-} ions involved in the NO_3^- ions. It is well known that although the ionic bonds dominate Na-O pairs, some covalent bonds are still involved in it. Moreover, with the enhancement of the covalent bonds the release of Na^+ ions from Na-O becomes more difficult. On the other hand, the amount of the covalent bonds involved in Na-O is not only determined by the intrinsic properties of the element Na and O but also by the situated environment of the combined O^{2-} ions and Na^+ ions. With regard to the tetragonal perovskite $PbTiO_3$, the larger number of covalent bonds may be presented in the Na-O pairs formed by the Na^+ ions with the O^{2-} ions situated at the (001) surfaces. When $NaNO_3$ is used as additive in the hydrothermal system for synthesis of the tetragonal perovskite $PbTiO_3$ crystals, in the present experiment, Na^+ ions are effectively bounded on the (001) surfaces by the enhanced covalent bonds. As a consequence, the deposition of the lead titanate species along the [001] directions is suppressed by the fastened Na^+ ions. The preferential deposition of the lead titanate species on the surfaces of (100) and (010) results in the single-crystalline tetragonal perovskite $PbTiO_3$ nanosheets with dominant (001) facets (Fig. 1b-d).

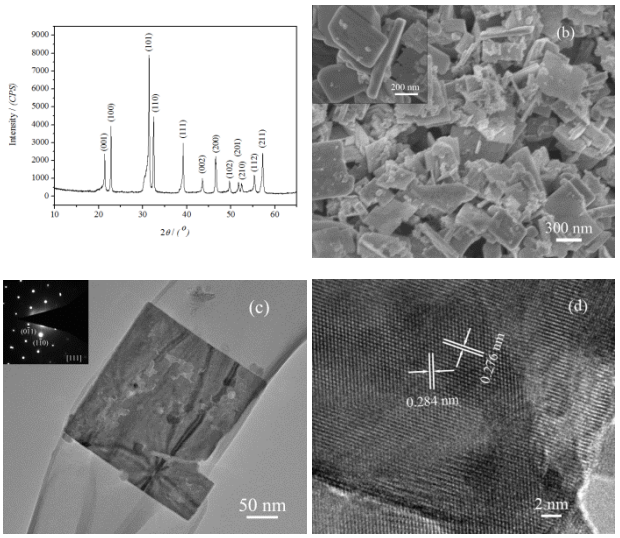

Fig. 2 (a) XRD pattern and (b) FESEM image of the hydrothermally synthesized perovskite lead titanate nanosheets fabricated with the addition of KNO_3 (b) is the magnified FESEM image of the $PbTiO_3$ nanosheets, (c) TEM image of one single $PbTiO_3$ nanosheet, (c) shows the SAED pattern taken from the whole single $PbTiO_3$ nanosheet, (d) HRTEM image of the as-prepared $PbTiO_3$ nanosheets

In order to verify the above proposed formation mechanism, KNO_3 and $LiNO_3$ were employed as additives in the hydrothermal system instead of $NaNO_3$, respectively. XRD and SEM results shown in Fig. 2 reveal that as in the case of the $NaNO_3$ addition, the introduction of KNO_3 also induces the formation of the $PbTiO_3$ nanosheets. Similarly, along with the nanosheets, a number of nanocrystallites also form (Fig. 2b). Thus, the broadened shoulders with the diffraction peaks are also observed in the XRD pattern (Fig. 2a). The regular SAED pattern as inset shown in Fig. 2c is taken from the corresponding single whole nanosheets and can be indexed as the incident electron beam along with [111] direction. Therefore, the obtained $PbTiO_3$ nanosheets in the presence of KNO_3 are single-crystal and dominated with (111) facets, not as the obtained in the presence of $NaNO_3$ dominated with (001) facets. Because the (10-1) and (-110) is perpendicular to the [111] direction, the fringes with intervals of 0.284 nm and 0.276 nm, which agree well with the spacing of (10-1) and (-110), are observed in the HRTEM image presented in Fig. 2d. However, when $LiNO_3$ is used instead of $NaNO_3$, the formation of the tetragonal perovskite $PbTiO_3$ phase is inhibited. After completing hydrothermal treatment, the obtained samples are composed of titanium and lead oxide nanoparticles without any lead titanate (Fig. S4).

It is well known that the three elements of Li, Na and K belong to the first main-group in the periodic table. However, they have different electro-negativity. With the element number increasing, the electro-negativity decline from 0.98 for Li to 0.93 and 0.82

for Na and K, respectively. Thus, Li-O pairs contain a larger number of covalent bonds than Na-O and K-O pairs. In view of the orientation and saturation condition of covalent bonds, the larger number of covalent bonds makes the release of Li^+ ions from Li-O pairs by ionization becomes more difficult than from Na-O and K-O pairs. When $LiNO_3$ is used as additive in the hydrothermal system, most of O^{2-} ions situated at the surface of the TiO_6 octahedrons are riveted by forming fast combined Li-O pairs. As a consequence, the combination of Pb^{2+} ions with the TiO_6 octahedrons to form lead titanate is suppressed. Thus, no lead titanate phases are checked out from the obtained samples but for titanium and lead oxides after hydrothermal treatment at the presence of $LiNO_3$ (Fig. S4).

On the other hand, because Na-O and K-O pairs contain a lower number of covalent bonds than Li-O pairs, the release of Na^+ and K^+ ions from Na-O and K-O pairs by ionization becomes much easier than that of Li^+ ions from Li-O pairs. Therefore, when the $NaNO_3$ and KNO_3 are used as additives instead of $LiNO_3$, a larger number of O^{2-} ions situated at the surfaces of the TiO_6 octahedrons become available by releasing Na^+ and K^+ ions to combine with Pb^{2+} ions for forming lead titanate species and further crystals. As a consequence, pure tetragonal $PbTiO_3$ perovskite samples are hydrothermally synthesized at the presence of $NaNO_3$ and KNO_3 (Fig. 1a and Fig. 2a).

However, due to the difference in elelctronegativity of the two elements of Na and K, the presence of KNO_3 induces the single-crystal tetragonal perovskite $PbTiO_3$ nanosheets with dominanat (111) facets not as the induced one with dominant (001) facets by the addition of $NaNO_3$. It has been demonstrated above that due to the cooperation of the intrinsic properties of the element Na and O and the situated environment of the O^{2-} ions, Na^+ ions are fast bounded on the (001) surfaces by the formed Na-O pairs with enhanced covalent bonds, which effectively suppresses the deposition of the lead titanate species on the (001) planes and induces the single-crystal tetragonal perovskite $PbTiO_3$ nanosheets with dominant (001) facets. When KNO_3 is used in the hydrothermal system instead of $NaNO_3$, due to the lower electro-negativity, which creates a lower number of covalent bonds in K-O pairs than that in Na-O pairs, the bounded K^+ ions on the (001) planes release much more easily compared to the bounded Na^+ ions on the (001) planes. The deposition of the lead titanate species on (001) surfaces is intensified. Nonetheless, because the (111) planes are the densest one in the tetragonal perovskite $PbTiO_3$ crystal structure, the ability of the O^{2-} ions situated at the (111) planes to capture electrons along [111] direction is weaker compared to other O^{2-} ions. The synergistic effects of the weaker capture ability of the O^{2-} ions situated at the (111) planes and the lower electro-negativity of K makes the formed K-O pairs of a larger number of covalent bonds. As a consequence, the deposition of the lead titanate species on (111) planes is suppressed and the single-crystalline tetragonal perovskite $PbTiO_3$ nanosheets with dominant (111) facets are hydrothermally synthesized (Fig. 2).

Conclusions

In summary, the single-crystalline tetragonal perovskite $PbTiO_3$ nanosheets with dominant (001) or (111) facets have been successfully synthesized by a conventional hydrothermal route assisted with $NaNO_3$ and KNO_3, respectively. Due to the difference in electro-negativity, Na^+ ions are fasten on the (001) surfaces, whereas K^+ ions are fast bounded on the (111) surfaces. Thus, in the presence of $NaNO_3$ the deposition of lead titanate species on (001) planes is suppressed, whereas in the presence of KNO3 the deposition on the (111) planes is inhibited, resulting in the single-crystal tetragonal perovskite $PbTiO_3$ nanosheets dominated with (001) or (111) facets, respectively. These nanosheets could be an ideal candidate structure for fundamental studies of nanoferroelectricity, piezoelectricity, and paraelectricity, especially for pursuing nonvolatile memory devices with higher storage density.

Acknowledgements

This work is supported by the National Natural Science Foundation of China under grant Nos. 61274004 and 51232006, and the Zhejiang Natural Science Foundation, China, under grant No. LY12B07007, and Key Science and Technology Innovation Team of Zhejiang Provice, China, under grant No. 2010R50013.

Notes and references

[a] *State Key Laboratory of Silicon Materials and Department of Materials Science and Engineering, Zhejiang University, Key Laboratory of Advanced Materials and Applications for Battery of Zhejiang Province, Hangzhou 310027, China. Fax: 86 571 87952341; Tel:86 572 8792341; E-mail: msegxu@zju.edu.cn*

[b] *Department of Mechanical and Materials Engineering, Queen's University, Kingston, Ontario K7L 3N6 Canada*

† Electronic Supplementary Information (ESI) available: Experimental details; XRD patterns, SEM images. See DOI: 10.1039/b000000x/

1 A. Name, B. Name and C. Name, *Journal Title*, 2000, **35**, 3523; A. Name, B. Name and C. Name, *Journal Title*, 2000, **35**, 3523.
1 O. Auciello, J. F. Scott, R. Ramesh, Phys. Today, 1998, 51, 22.
2 W. S.Yun, J. J.Urban, Q. Gu, H. Park, Nano Lett., 2002, 2, 447.
3 J. E. Spanier, A. M. Kolpak, J. J. Urban, I. Grinberg, L. Ouyang, W. S. Yun, A. M. Rappe, H. Park, Nano Lett., 2006, 6, 735.
4 R. Ma, T. Sasaki, Adv. Mater., 2010, 22, 5082.
5 J. N. Coleman, M. Lotya, A. O' Neill, S. D. Bergin, P. J. King, U. Khan, K. Young, A. Gaucher, S. De, R. J. Smith, I. V. Shvets, S. K. Arora, G. Stanton, H. Y. Kim, K. Lee, G. T. Kim, G. S. Duesberg, T. Hallam, J. J. Boland, J. J. Wang, J. F. Donegan, J. C. Grunlan, G. Moriarty, A. Shmeliov, R. J. Nicholls, J. M. Perkins, E. M. Grieveson, K. Theuwissen, D. W. McComb, P. D. Nellist, V. Nicolosi, Science, 2011, 331, 568.
6 R. E. Schaak, T. K. Mallouk, Chem. Mater., 2002, 14, 1455.
7 R. Ma, Z. Liu, L. Li, N. Iyi, T. J. Sasaki, Mater. Chem., 2006, 16, 3809.
8 Y. Ebina, K. Akatsuka, K. Fukuda, T. Sasaki, Chem. Mater., 2012, 24, 4201.
9 K. S. Novoselov, A. K. Geim, S. V. Morozov, D. Jiang, Y. Zhang, S. V. Dubonos, I. V. Grigorieva, A. A. Firsov, Science, 2004, 306, 666.
10 G. Eda, M. Chhowalla, Adv. Mater., 2010, 22, 2392.
11 G. Xu, Z. H. Ren, P. Y. Du, W. J. Weng, G. She, G. R. Han, Adv. Mater., 2005, 17, 907.
12 Z. H. Ren, G. Xu, Y. Liu, X. Wei, Y. H. Zhu, X. B. Zhang, G. L. Lv, Y. W. Wang, Y. W. Zeng, P. Y. Du, W. J. Weng, G. Shen, J. Z. Jiang, G. R. Han, J. Am. Chem. Soc., 2010, 132, 5572.
13 G. Xu, W. B. He, Y. G. Zhao, Y. Liu, Z. H. Ren, G. Shen, G. R. Han, CrystEngComm, 2011, 13, 1498.
14 E. P. Stambaugh, Hydrothermal precipitation of high-quality oxides, presented at the SME-AIME Fall Meeting, St. Louis, MO, 1977.
15 J. A. Venables, Introduction to surface and thin film processes, Cabridge University Press, Cambridge 2000, P.4.

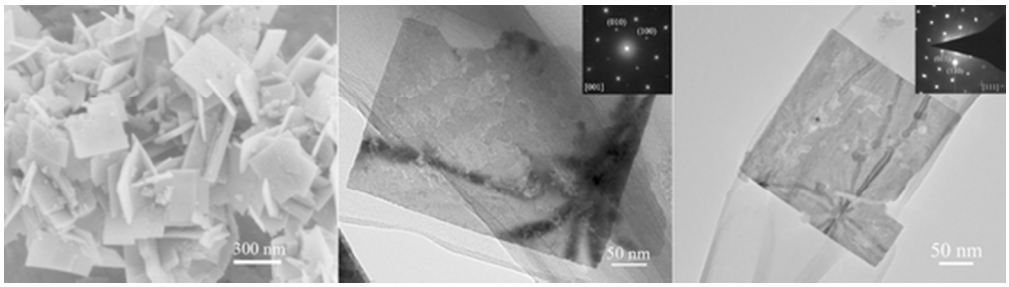

Due to the difference in electronegativity, Na+ ions are fastened on (001) planes, whereas K+ ions on (111) planes, resulting in the PbTiO3 nanosheets dominant with (001) or (111) facets, respectively.
25x6mm (600 x 600 DPI)